TECTONICS AT THE INTERSECTION OF THE EAST PACIFIC RISE WITH TAMAYO TRANSFORM FAULT

TAMAYO TECTONIC TEAM
(D. G. GALLO[1], W. S. F. KIDD[2], P. J. FOX[1], J. A. KARSON[3], K. MACDONALD[4], K. CRANE[5], P. CHOUKROUNE[6], M. SEGURET[7], R. MOODY[2], and K. KASTENS[5])

(Accepted 20 August, 1983)

Abstract. During the Fall of 1979, a manned submersible program, utilizing DSRV ALVIN, was carried out at the intersection of the East Pacific Rise (EPR) with the Tamayo Transform boundary. A total of seven dives were completed in the vicinity of the EPR/Tamayo intersection depression and documented the geologic relationships that characterize the juxtaposition of these types of plate boundaries. The young volcanic terrain of the EPR axis can be traced into and across the Tamayo Transform valley but becomes buried by sedimentary talus that is being shed from sediment scarps along the unstable sediment slope that defines the north side of the intersection depression. Within 4 km of the transform boundary, the dominant trend (000°) of the fissures and faults that disrupt the rise-generated volcanics is markedly oblique to the regional direction of sea floor spreading (120°). Since no evidence was found to suggest that these structures accommodate significant amounts of strike-slip displacement, they are taken to reflect a distortion of the EPR extensional tectonic regime by a transform generated shear couple. The floor of the Tamayo Transform valley in this area is inundated by mass-wasted sediment, and the principal transform displacement zone is characterized at the surface by a narrow (< 1.5 km) interval of fault scarps in sediment that trends parallel with the transform valley. Extrapolated to the west, this zone links with zones of transform deformation investigated during earlier submersible studies (CYAMEX and Pastouret, 1981). Evidence of low-level hydrothermal discharge was seen at one locality on the EPR axis and at another 8 km west of the axis at the edge of the zone of transform deformation.

1. Introduction

Investigations of the morphotectonic fabric developed proximal to ridge-transform intersections (Crane, 1976; Lonsdale, 1978; Searle, 1979; Macdonald *et al.*, 1979; OTTER, 1984; Karson and Dick, 1983) indicate that the topographic trends in these regions are oblique to both the ridge axis and the transform fault. Two different mechanisms have been suggested to account for the presence of this obliquity. In one scheme, oblique topographic elements evolve as the product of a system of strike-slip or oblique-slip faults referred to as Riedels and anti-Riedels (Tchalenko, 1970; Riedel, 1929), or secondary shear structures (McKinstry, 1953;

[1] Graduate School of Oceanography/URI, Narragansett, RI 02882, U.S.A.
[2] Department of Geological Sciences, SUNY at Albany, Albany, NY 12222, U.S.A.
[3] Woods Hole Oceanographic Institution, Woods Hole, MA 02543, U.S.A.
[4] Department of Geological Sciences, U.C.S.B., Goleta, CA 93106, U.S.A.
[5] Lamont-Doherty Geological Observatory of Columbia University, Palisades, NY 10964, U.S.A.
[6] Laboratoire de Geologie Structural, B. P. No. 25A, 35031 Rennes Cedex, France.
[7] Universite des Sciences et Techniques de Languedoc, Place Eugene Bataillon, 34060 Montpellier Cedex, France.

Marine Geophysical Researches **6** (1984) 159–185. 0025-3235/84/0062-0159 $04.05

Chinnery, 1976) that are known to form within and along zones of shear. If these structures are responsible for the development of the oblique trending fabric found at ridge-transform intersections, then evidence for strike-slip displacement in those areas should be apparent. An alternative explanation suggests that the oblique topographic elements reflect faults with dominant dip-slip displacements, that form near the ridge-transform boundary where the shear couple produced by the transform distorts the regional stress field associated with the ridge-axis (Courtillot *et al.*,1974; Crane, 1976; Lonsdale, 1978; Gallo *et al.*, 1980; Searle, 1979; Macdonald *et al.*, 1979).

The resolution of conventional underway or deep-towed geophysical tools is not adequate to determine the sense of displacement across faults that characterize ridge-transform intersections and the focus of our ALVIN investigation was to use the high-resolution capabilities of a submersible to establish the tectonic character of a ridge-transform intersection and to document the effects of the Tamayo Transform boundary upon the structural and geochemical processes responsible for the generation of the oceanic lithosphere along the East Pacific Rise (EPR; Tamayo Scientific Team, 1980a, b, c). A complementary surface ship program using R/V GILLISS mapped (by using a conventional 12 kHz echo sounder) and systematically sampled (conventional dredging) the EPR axial volcanic terrain from the EPR/Tamayo intersection to a distance 40 km south of the Tamayo transform boundary. The surface ship program was designed to provide a geochemical test for the deep-seated thermal effects of the Tamayo Transform boundary upon the generation of oceanic lithosphere along this segment of the EPR. The results of the dredging program are mentioned briefly in this paper and are presented in detail in a separate publication (Bender *et al.*, 1984).

2. Regional Setting of the Tamayo Transform and General Tectonic Framework

The Tamayo Transform represents the southernmost strike-slip plate boundary segment withing the gulf of California (Larson *et al.*, 1968, 1972; Figure 1). It links the Gulf Rise with the East Pacific Rise (EPR), and roughly parallels the theoretical slip-line between the Pacific and North American plates. The Tamayo transform domain is 80 km long and 35 km wide, strikes WNW – ESE (120°), and is characterized by right-lateral relative motion of approximately 6.0 cm $yr.^{-1}$ A bathymetric map compiled by Kastens *et al.* (1979) indicates that the transform domain is comprised of 3 first-order morphotectonic elements: a northern trough, a southern trough and an intervening median ridge (Figure 2A). The southern trough is about 10 km wide, and 60 km long. The floor of the trough is flat and its margins are outlined by approximately the 2800 m isobath. A 100 to 400 m high elongate ridge defines a central lineament along the transform valley axis and runs the length of the transform. At its western end this median ridge is broad (8 km), and high, standing 400 m above the flanking troughs but towards the east it loses

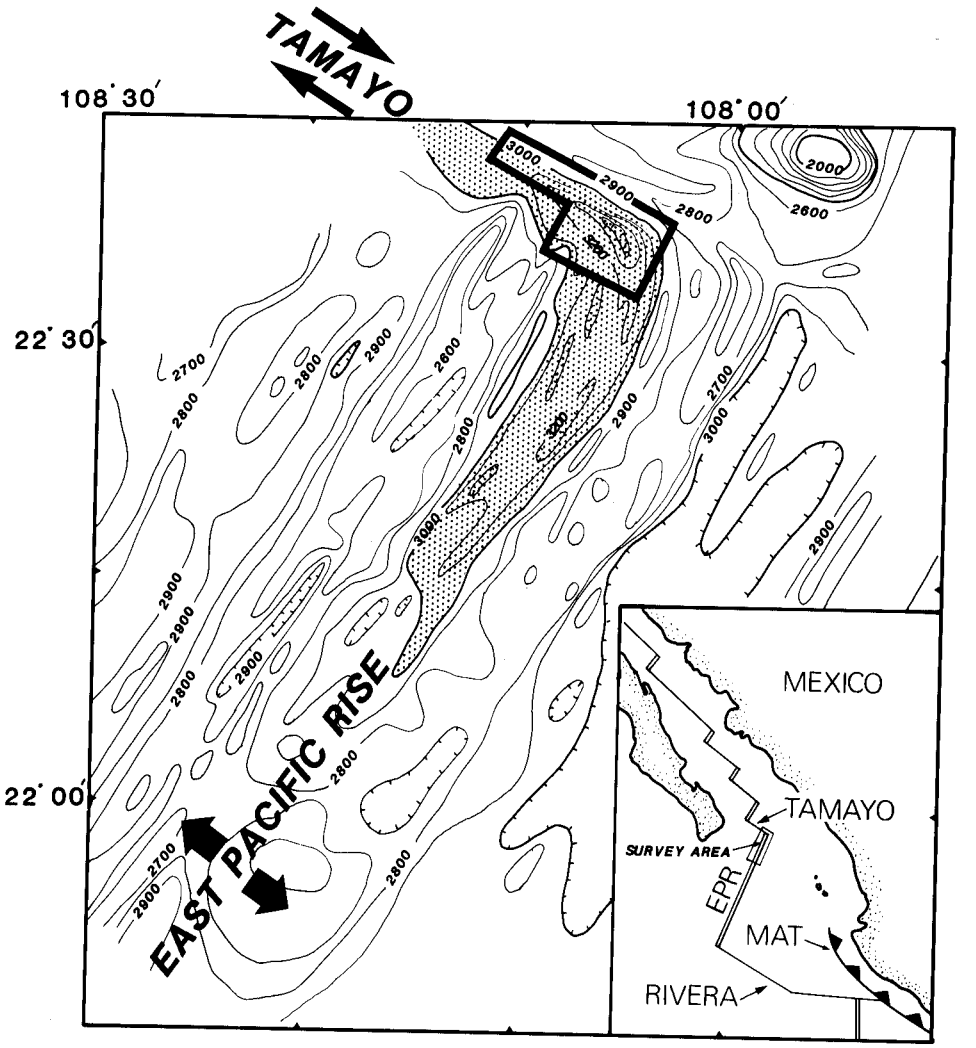

Fig. 1. Bathymetry of the East Pacific Rise (EPR) and the Tamayo Transform; regional location given in insert (MAT – Middle America Trench). Within about 30 km of the Tamayo Transform, the EPR axis gradually develops a well-defined rift valley (inner-valley floor shaded). Location of ALVIN dives at the EPR-Tamayo intersection shown by boxed area. Bathymetry compiled from data collected by R/V GILLISS, and this cruise (uncorrected meters).

definition and relief. The north trough is clearly defined by the 2900 m isobath, and is approximately 15 km wide. Seismic reflection data reveal that flat lying, undisturbed and acoustically reverberant sediments partially fill the north and south troughs with thicknesses ranging from 100 to 300 m (Kastens *et al.*, 1979). These data also show that diapir-like structures protrude into the sediment of both the northern and southern troughs. Several of the diapiric bodies deform reflectors

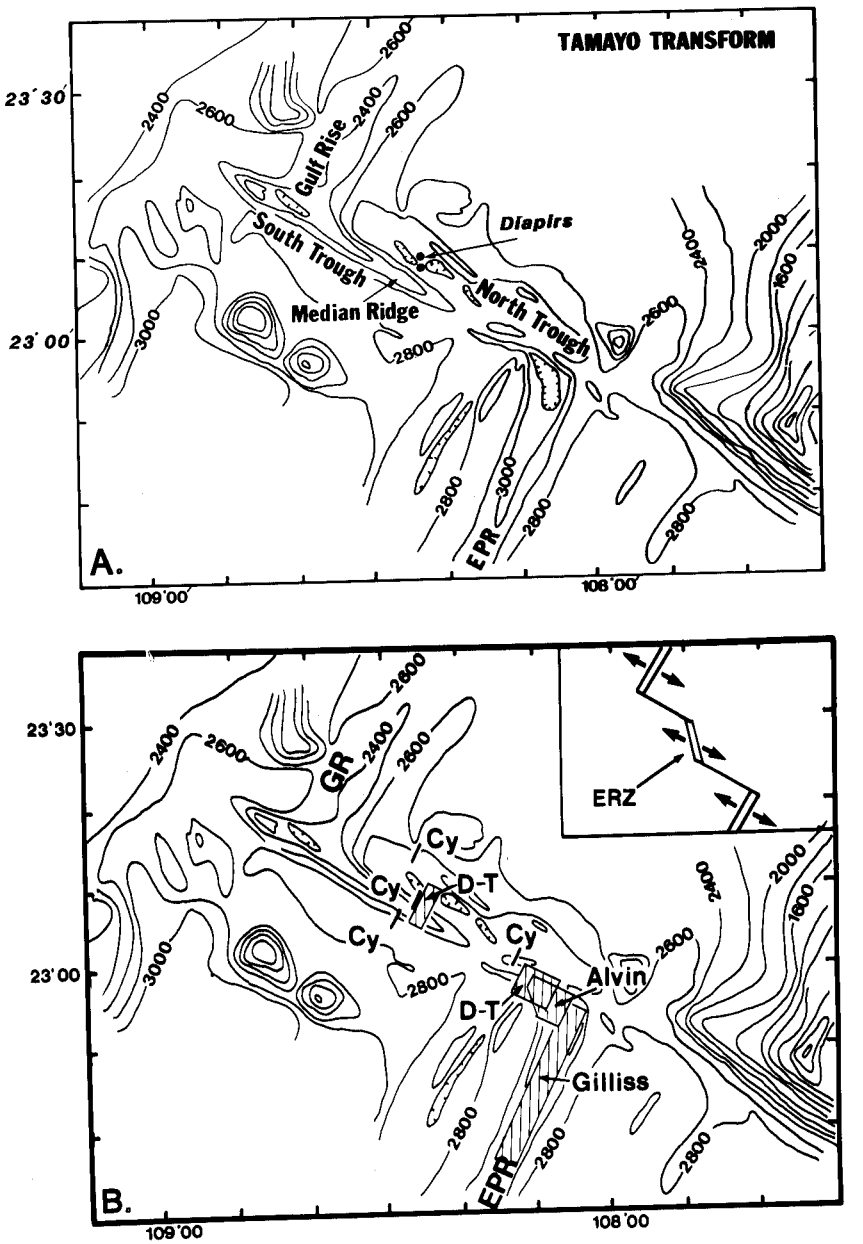

Fig. 2A. Morphotectonic province of the Tamayo Transform (after Kastens *et al.*, 1979). The Tamayo Transform is characterized by right- lateral strike-slip displacement of about 6cm/yr. Total transform offset is approximately 80 km. (B) Location of previous detailed geologic investigations of the Tamayo Transform boundary. GR – Gulf Rise; EPR – East Pacific Rise; CY – CYANA dives (CYAMEX and Pastouret, 1981); D–T – Deep Tow Study Areas (Macdonald *et al.*, 1979); ALVIN – ALVIN dive areas (this paper); and GILLISS – Dredging program (this paper, and Bender *et al.*, 1983). Also shown in insert is the kinematic interpretation of the Tamayo Transform showing two strike-slip segments linked by an extensional relay zone (ERZ; Macdonald *et al.*, 1979; CYAMEX and Pastouret, 1981).

at shallow sub-bottom depths by punching up through or bowing up the horizontal strata.

Surface ship bathymetric surveys (Lewis *et al.*, 1983; Lewis, 1979) and a deep-towed geophysical-package profile (Macdonald *et al.*, 1979) show that the morphotectonic character of the EPR axis changes gradually, over a distance of 50 km towards the transform, from a broad and subtly rifted topographic swell into a well-defined valley exhibiting classic Atlantic-type rift valley morphology (Figure 1). Seismic refraction studies by McClain and Lewis (1980) suggest that the thickness of the oceanic crust created along the EPR thins by 2 to 3 km as the Tamayo Transform is approached. Both of these observations are interpreted to reflect the thermal influence of the Tamayo Transform boundary upon the deep-seated processes responsible for the generation of oceanic lithosphere (Fox and Gallo, 1984).

Two areas of the Tamayo Transform have been studied in detail using a deep-towed geophysical package (Macdonald *et al.*, 1979; Figure 2B). The first survey area lies along a N–S line at the center of the transform. Along the transect, which crossed parts of both troughs and the median ridge, shallow reflectors are undisturbed and conformable to the sea floor except in the center of the northern trough where a diapir-like body punches through the sediment overburden uplifting a cap of acoustically reverberant sediments.

The second region investigated by Macdonald and others (1979) lies a few kilometers to the west of the Tamayo-EPR intersection (Figure 2B). The survey shows that the ridge-transform intersection is characterized by an elongate depression that extends westwards along a strike of WNW–ESE (115°). The floor of the depression is comprised of sparsely sedimented volcanic terrain proximal to the EPR but is covered by a sedimentary blanket farther to the west. The north side of the depression is bounded by a 300 to 400 m high, south facing slope which dips 10° to 20° towards the axis of the depression. The smooth regional gradient of the slope is disrupted by steep scarps with individual relief of a few tens of meters and with continuity along a strike of several hundreds of meters to a few kilometers. The southern flank of the depression is a 500 m high north facing ediface consisting of a series of steeply dipping scarps exhibiting trends both oblique (345°) and parallel to the strike of the East Pacific Rise axis (030°). Macdonald and others (1979) interpret the scarps that disrupt the northern slope of the depression to represent a narrow (< 1 km) principal transform displacement zone (PTDZ). The ridge-axis parallel and oblique structures that bound the depression to the south can be traced to within a few hundred meters of the PTDZ suggesting to Macdonald *et al.*, (1979) that the zone of decoupling between the extensional regime of the rise axis and the strike-slip environment of the transform is very narrow. The oblique trends were interpreted to be the product of a shear couple that forms at the EPR-Tamayo intersection.

Four dives by the French submersible CYANA were located within the Tamayo Transform (Figure 2B): one dive, positioned along the north side of the northern

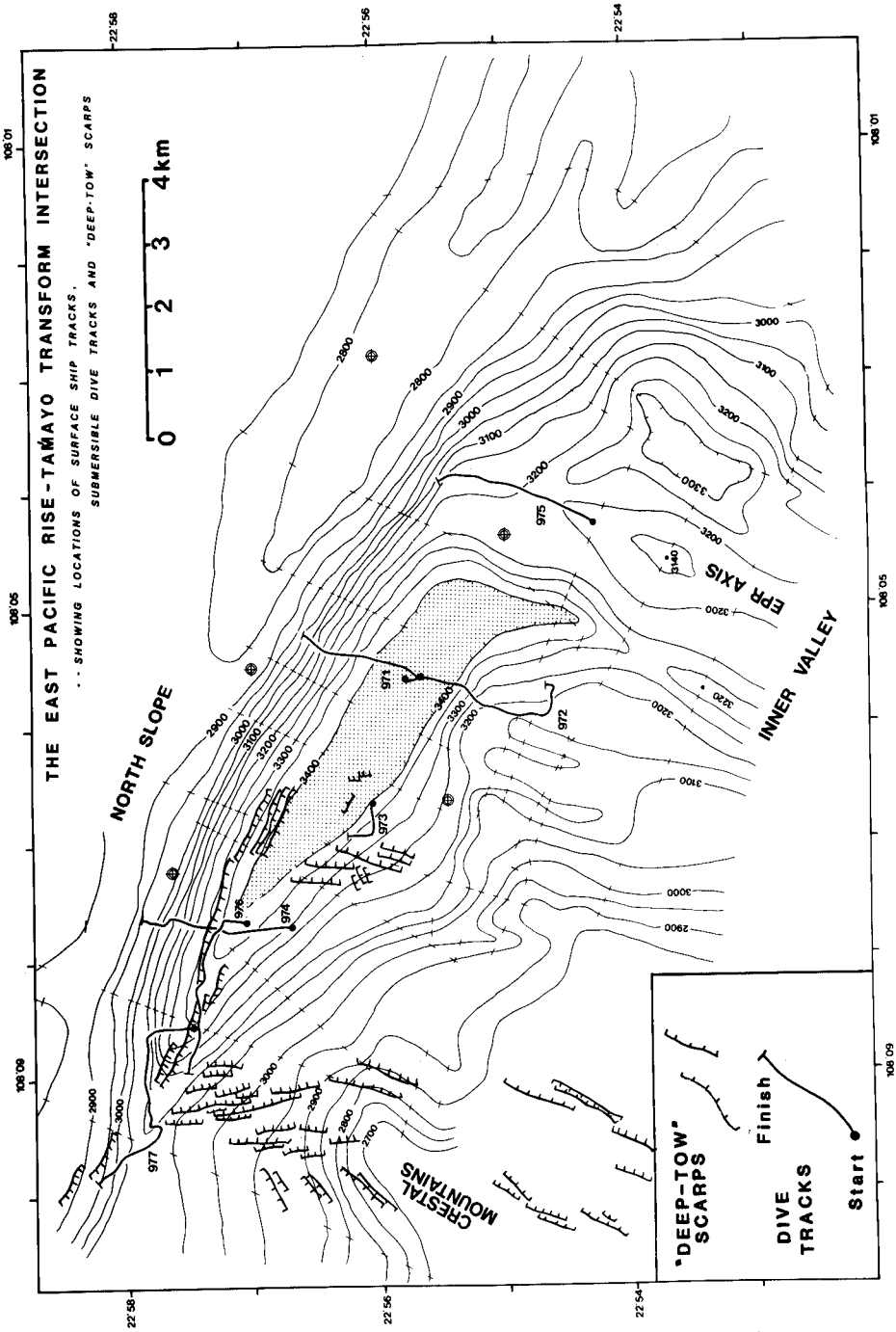

Fig. 3. Bathymetry of the EPR-Tamayo Intersection (location given by Figures 1, 2B) and position of ALVIN dive tracks (971–977). Deep-tow lineaments, interpreted to be fault scarps, are shown as lines with hachures in the downslope direction. Bathymetry by 12 kHz echo sounding from R/V LULU, this cruise. Note that only part of this area has deep-tow side-scan sonar coverage (see Macdonald *et al.*, 1979).

trough west of the diapir field surveyed by Macdonald *et al.*, (1979), crossed a narrow (< 500 m) zone of recently deformed sediment with structures striking 115°; two dives which traversed the median ridge documented that there is no evidence for recent tectonism in this region; one dive, located towards the eastern end of the median ridge, found a 500 m wide zone of recent tectonism defined by structural lineaments striking 120° (CYAMEX and Pastouret, 1981).

The combined results from surface-ship surveys, deep-towed geophysical investigations and submersible observations suggest that the PTDZ at various locations along the transform is relatively narrow (< 1 km) and that the zone of strike-slip motion is not continuous along strike down the length of the Tamayo transform but rather appears to be offset by an extensional relay zone characterized by presumed serpentinite diapirs (Macdonald *et al.*, 1979; CYAMEX and Pastouret, 1981; Figure 2B, Insert).

3. The Geology of the EPR-Tamayo Intersection: Sea Floor Observations

Seven dives with the DSRV ALVIN were completed at the eastern end of the Tamayo Transform boundary, proximal to its intersection with the axis of the EPR (Figures 2B, 3). Four dives (971, 972, 973, 975) were located in the immediate vicinity of the EPR/Tamayo intersection (Figures 3, 4, 5) and three dives (974, 976, 977) were positioned 6 to 10 km to the west along the intersection depression (Figures 3, 6, 7). These dives, in whole or in part, traversed the morphotectonic zones described for the intersection area by Macdonald *et al.*, (1979). These zones include the EPR rift valley floor (Dive 975), the EPR/Tamayo intersection deep (Dives 971, 972, 973), the western rift valley wall of the EPR (Dive 972), and the northern wall of the intersection depression (Dives 971, 974, 976, 977; Figure 3).

3.1. The rift valley floor

Visual observations from submersible ALVIN confirm that the rift valley floor, in the vicinity of the Tamayo Transform fault, is comprised of glass encrusted, lightly sediment-dusted volcanic terrain that has been only slightly disrupted by tectonic activity (fissuring and faulting; Figures 8A, B). The bathymetric map of this area (Figure 3; see also Figure 5 of Macdonald *et al.*, 1979) show that the axis of the EPR, just south of the Tamayo Transform boundary, is dominated by a 1–2 km wide topographic high, whose crest stands nearly 100 m above the surrounding rift valley floor. As this axial-high is traced northward, towards the Tamayo Transform boundary, it appears to taper gradually both in width and height. Visual observations of the northern end of this feature (Dive 975; Figures 3, 4, 5D) show that it is composed of numerous constructional volcanic mounds, haystacks, and steep (>60°) lava tube-covered edifices. The maximum relief of these features (mounds, ridges, etc.) is typically less than a few tens of meters and the mounds themselves are characterized by a predominance of fresh, completely

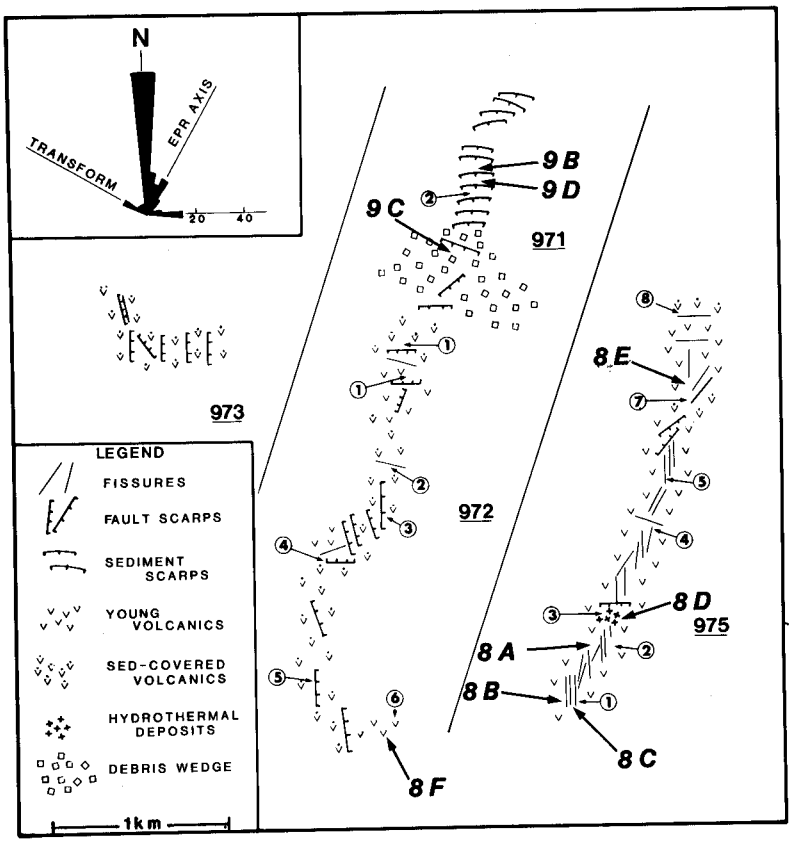

Fig. 4. Structural lineaments and geology of the EPR-Tamayo intersection (Dives 971, 972, 973, 975), locations given by Figure 3. Note that the dominant trend of brittle structures (faults, fissures) within the EPR volcanic basement is N–S (000°, see rose diagram insert) oblique by 30° to the regional EPR trend but scarps in sediment, not included in rose diagram (Dive 971–northern end) trend subparallel to the trend of the Tamayo Transform valley (120°). Circled numbers indicate sampling locations. Bold numbers indicate locations of photos given in Figures 8 and 9. See text for further discussion.

glassy pillow and tubular lavas. Extensive sheet or pounded flows were not observed on this dive but localized occurences are suggested by a broad, thin (2–3 cm) veneer of basalt that partially buries pillow forms (Figure 8C). The youthfulness of this volcanic terrain is shown not only by a paucity of pelagic sediment cover (> 2 cm) in this area of relatively high sedimentation rate, but also by the presence of delicate ornaments (e.g. glass buds) on pillows and thick, unpalagonitized glass rinds on pillow surfaces. Furthermore, at one location next to a fissure, a fluffy yellow-white amorphous chemical precipitate (iron-rich montmorillonite to nontronite, M. Mottl, personal communication) was observed partially blanketing very heavily manganese-coated pillows and is interpreted to be of low-temperature hydrothermal origin (Figure 8D). It is important to note that the number of fissures observed in this area (61) is much greater than the number of faults (5) indicating that horizontal extension, without vertical displacment

along fault scarps, is the primary deformational process acting here. Fissures range up to 4 m wide but most are about 1–2 m wide. Many of them expose sections through pillows with a chalky film of vein material on the broken surfaces. The dominant trend of the fissures and faults in this region is N–S (000°); oblique by 30° (counterclockwise) to the regional trend (030°) of the EPR axis (Figure 4 insert). None of the structures (faults/fissures) observed in this terrain are laterally continuous for more than about 50 m and none develop significant amounts of vertical relief (< 5 m). Typically, the base of fault scarps are characterized by sediment-free talus ramps, composed of abundant cobble-sized and larger pillow and tube fragments. The youthful appearance and extent of the talus indicate that mass-wasting processes tend to smooth any tectonically created relief soon after it is generated.

Curiously, as the axial volcanic high approaches the northern side of the intersection depression the relief and continuity of the high appear to diminish but the amplitude of the hummocky volcanic terrain (i.e. the relief of individual volcanic mounds, etc.) increases considerably and the average depth to basement decreases (Dive 975, Figure 5D). Tube-draped mounds and ridges in this area exhibit relief on the order of 50 m to 70 m and their flanks develop slopes that are locally steeper (40° to vertical) than those found along the first half of Dive 975 immediately to the south. In addition to the increased amplitude of individual volcanic-constructional elements, several other interesting contrasts emerge between the terrain seen during the first and second phase of Dive 975. Sharp breaks in slope, well developed sediment-free talus ramps (Fig 8E; > 10 m high), and scarp faces exposing freshly truncated pillows and tubes signify that faulting has been recent and that significant dip-slip displacement (10–30 m) has occurred along the faults in this area. As opposed to the predominance of fissuring over faulting seen during the first half of Dive 975, fissures were rarely seen during the second half. The few fissures that were observed have trends that are subparallel to that of the Tamayo Transform (120°; Figure, 4), significantly different from the N–S trend observed on the first part of Dive 975, and the dominant 030° structural trend along the EPR axis farther to the south.

3.2. Western rift valley wall

The only large throw (> 40 m) faults observed within or proximal to the EPR/Tamayo intersection area are a set of east-facing faults scarps traversed by Dive 972 (Figures 3, 4, 5B). These structures exist in lithosphere that is inferred to be approximately 100000 yr old and, based on our detailed bathymetric maps (Figures 1, 3) and on the Deep Tow bathymetric profile across the EPR (Macdonald *et al.*, 1979), are interpreted to represent the base of the EPR inner rift valley western wall. The bathymetric map (Figure 3) and dive profile (Figure 5B) suggest that this wall begins at about the 3400 m contour and shoals to about 3100 m. Dive 972 traversed up, along, and then partially down a portion of the western wall and documented that the observed 250 m relief is the product of

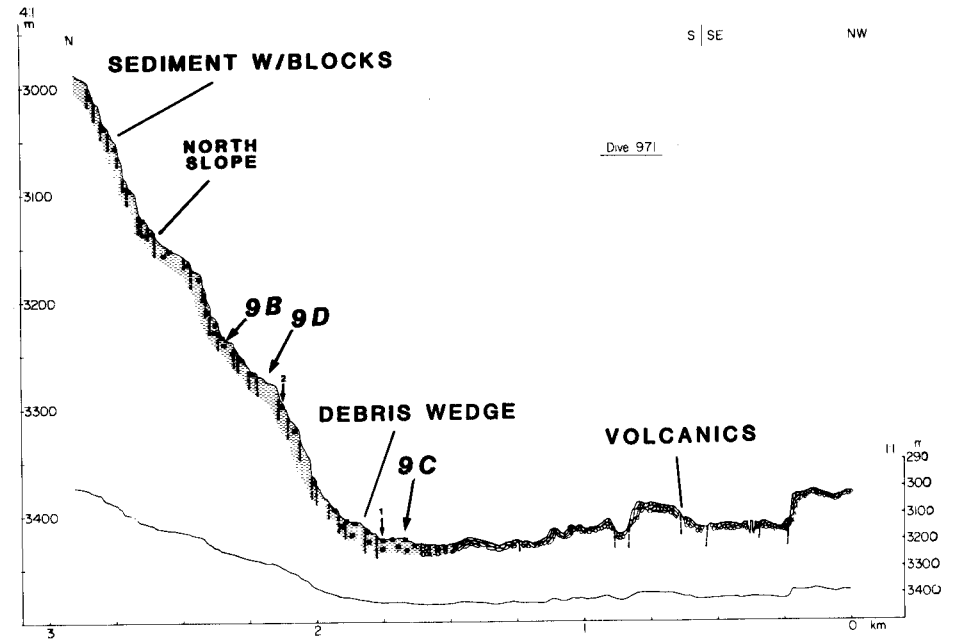

A.

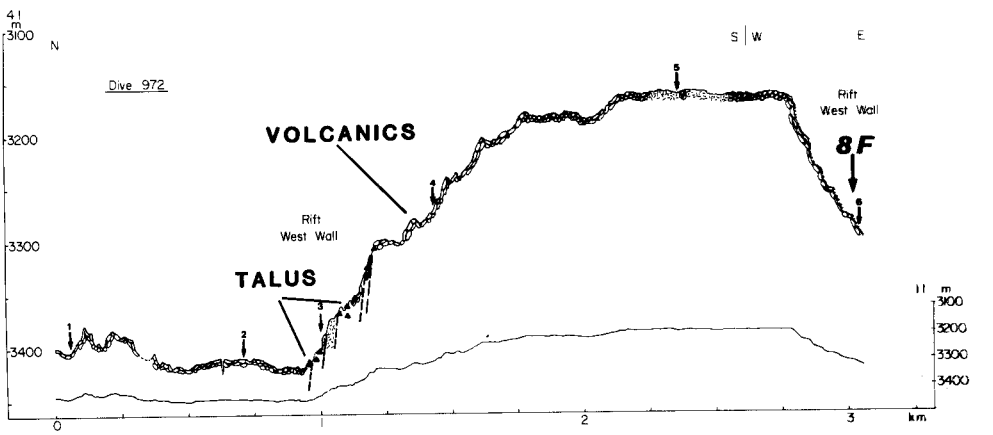

B.

several fault scarps which are laterally continuous for at least 1.5 km and have trends at the dive location of approximately 000°; that is, parallel with the local dominant fault and fissure trend of the EPR inner valley floor and significantly oblique to the regional trend of the EPR axis (030°; Figures 3, 4, 5B). Two of these faults expose truncated pillows and tubes and are characterized by sediment-free talus ramps that contain both massive and pillow basalt fragments. The larger throw faults at the base of the western wall also expose massive basalt sequences up to 50 m thick which, in places, show well-developed columnar jointing. These

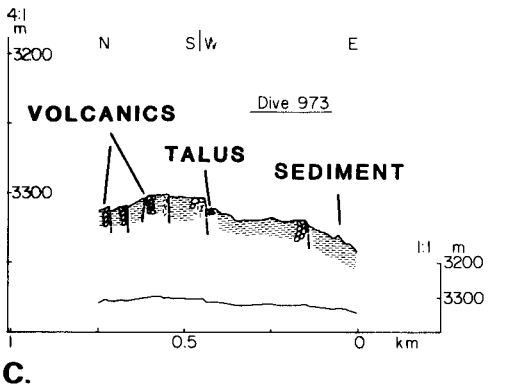

C.

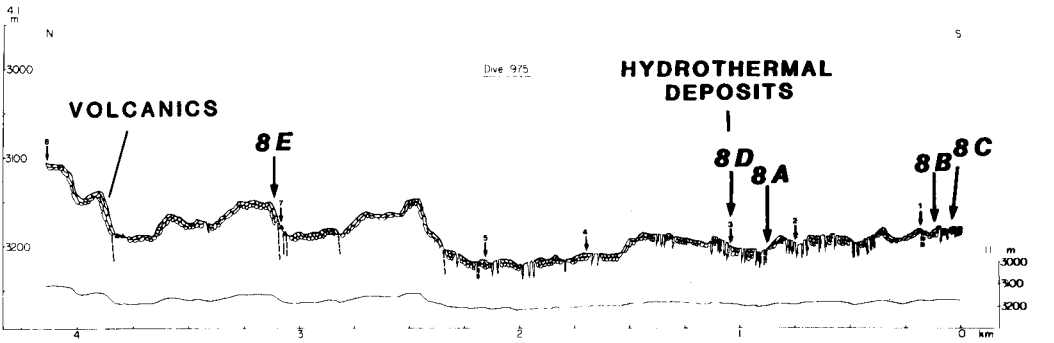

D.

Fig. 5A–D. Geologic profiles and sampling location numbers above profiles) along Dives 971, (A), 972 (B), 973 (C), 975 (D) respectively (locations shown by Figure 3). 4:1 and 1:1 profiles are given for each dive. Symbols used for geology are identified for each profile. Bold numbers indicate locations of photos given in Figures 8 and 9.

massive layers are interpreted to represent ponded flows and/or sills interlayered with the pillowed flows. Although it is clear that the large throw faults of the western wall reflect the onset of a regime in which tectonism dominates over the processes of volcanism, we found evidence showing that some volcanism has occurred at or near the top of the western rift valley escarpment, slightly off the axis of the EPR. In both upward and downward traverses of Dive 972, the steep uppermost portion of the western wall is draped with unbroken tubular lavas that appear to have been erupted from the top or from a location near the top of the wall (Figure 8F). This terrain of the upper part of the western wall is completely sediment-free and covered with glass-encrusted tabular lava forms, as shown by visual observations and samples recovered. West of these young pillows covering the upper part of the inner rift wall, the terrain is a gently undulating bench, exposing markedly more heavily sediment-covered (1–10 cm) pillows and sheet-type flows, including one small collapse pit.

3.3 The EPR-Tamayo intersection depression

Observations made during Dives 971 and 972 document that, with the exception of a thin (< 3 cm) veneer of hemipelagic sediment, a similar terrain to the EPR axial high exists three kilometers west of it along the floor of the intersection depression (Figures 3, 4, 5A, B). Based on a half-spreading rate of 30 mm yr^{-1} (Larson *et al.*, 1968), the volcanic terrain seen in this area should be approximately 100000 years older than that seen along the Dive 975 traverse; judging by the appearance of the lavas, the surface flows are much younger than this. As was observed during the second half of Dive 975, high-amplitude (> 20 m) volcanic mounds are present, and fissures are conspicuously scarce, although the few observed strike subparallel to the Tamayo Transform trend (120°).

Five kilometers west of the EPR axial volcanic high, the hummocky ridge-generated volcanic terrain of the intersection depression is overlain by a veneer of sediment several centimeters thick (Dive 973; Figures 3, 4, 5C). Based on the calculated 30 mm yr^{-1} half-rate of seafloor spreading, volcanic basement in this area is estimated to be on the order of 165000 years old. The sea floor observed in this region has subtle relief consisting of a gentle southeast-sloping sediment surface broken only by a few small (< 10 m high) N–S trending, east-facing scarps and ridges. The sediment cover is pock-marked by abundant worm-tracks, burrows and other indicators of active bioturbation. Dish-shaped depressions (< 1 m deep and usually < 50 cm in diameter) were observed and interpreted to be locations where unconsolidated sediment has drained, like sand in an hour-glass, either into voids within the underlying volcanic tunnel and tube systems, or into open fissures.

Although the oceanic crust seen along Dive 973 is 165000 yr older than that observed during Dive 975 and 65000 yr older than that observed during Dives 972 and 971, there is evidence to suggest that some structures observed in this area are tectonically active. In a few locations, several N–S scarplets (10–30 cm high, 10–15 m long) were seen within the sediment cover. The scarp-faces are near vertical and scarred by vertical striae suggestive of recent dip-slip motion. Masswasted debris is absent from the base of these scarps and indicates relatively recent formation. Also, near the end of Dive 973, a N–S trending graben-like structure was observed (5–7 m wide 2–3 m deep). The walls of this graben expose both truncated pillow and massive basalt. The sediment cover along the floor of the graben is littered with angular, sediment-free basalt fragments and boulders (0.5–1 m in diameter) suggesting some recent tectonic activity. However, the largest (~ 10 m high) N–S scarp seen on this dive showed sediment-blanketed manganese-veneered talus at its foot, demonstrating no recent activity along it.

At two locations along the intersection depression (Dives 976, 977; Figures 3, 6, 7B, 7C) topographic ridges of volcanic rock emerge from the > 1 m thick sediment cover that blankets the deepest portion of the depression. These basalt ridges trend NNW–SSE and WNW–ESE and are characterized by a gently dipping

west-facing slope and steep east-facing scarps that can be as high as 50 m (Dive 977, Figures 6, 7C). The steep scarps expose mostly manganese veneered angular basalt talus blocks and minor amounts of massive basalt outcrop (Figure 9A). Degraded pillow forms were observed at the tops of these scarps. The scanning sonar system (CTFM) of ALVIN shows that the largest of these features (Dive 977; Figures 6, 7C) is laterally continuous over a distance of at least 1.5 km and other ridges were traced along strike for distances of 500 m. All of the scarps seen in older terrain appear to be tectonically inactive; the talus piles are blanketed by sediment, the fragments are manganese veneered, and individual fragments of talus are in places welded together by manganese encrustation.

3.4. The northern side of the intersection depression

The northern boundary of the EPR/Tamayo intersection depression is defined by a steep, south-facing slope that rises abruptly above the elongate closed-contour depression creating between 300 to 600 m of relief (Figure 3). Four dives (971, 974, 976, 977; Figures 3, 4, 5, 6, 7) traveled either up, or up and along the slope in order to investigate its tectonic character and, in particular, to examine the 115° trending scarps that were thought to represent the location of the principal transform displacement zone (PTDZ; Macdonald *et al.*, 1979).

As the base of the northern slope is approached on Dive 971 (Figures 3, 4), the relief of the hummocky, EPR volcanic terrain becomes first gradually, and then rapidly, subdued by a progressively thickening wedge of sediment that has apparently been shed from localities on the south facing slope. The distal end of this wedge consists of fine-grained, muddy sediment that blankets the volcanics. The proximal part and the bulk of this sedimentary wedge is composed of blocks and clods of variably consolidated, muddy to arenaceous sediment that, in all cases, are seen to lie within a matrix of similar sediment (Figures 9B, 9C). At one location clam shells were seen mixed in with and partially buried by the sediment. This sediment wedge is about 400 m wide on Dive 971; the part consisting of exposed blocks occupies about 300 m of this total. No firm evidence of faults cutting the chaotic sedimentary wedge deposited at the base of the sediment slope was seen.

Observations from Dive 971 (Figure 5A) show that near its base, above the sediment wedge, the south-facing slope of the north flank of the intersection trough is comprised of numerous small amplitude (< 5 m), closely spaced (< 20 m) scarps in sedimentary material. These features are very steep (70° to 90°), dip towards the south, and are interpreted to be the surface manifestations of active fault scarps. Towards the west (Figures 6, 7; Dives 974, 976, 977) the character and general orientation of the scarps remains the same but the width of the zone containing well-defined scarps is much less even though the density of scarp distribution increases. All of the scarps seen along the sediment slope occur within poorly to well-consolidated sediments (Figure 9D), and in no case was igneous basement definitely recognized. At one location on Dive 971, however, ALVIN

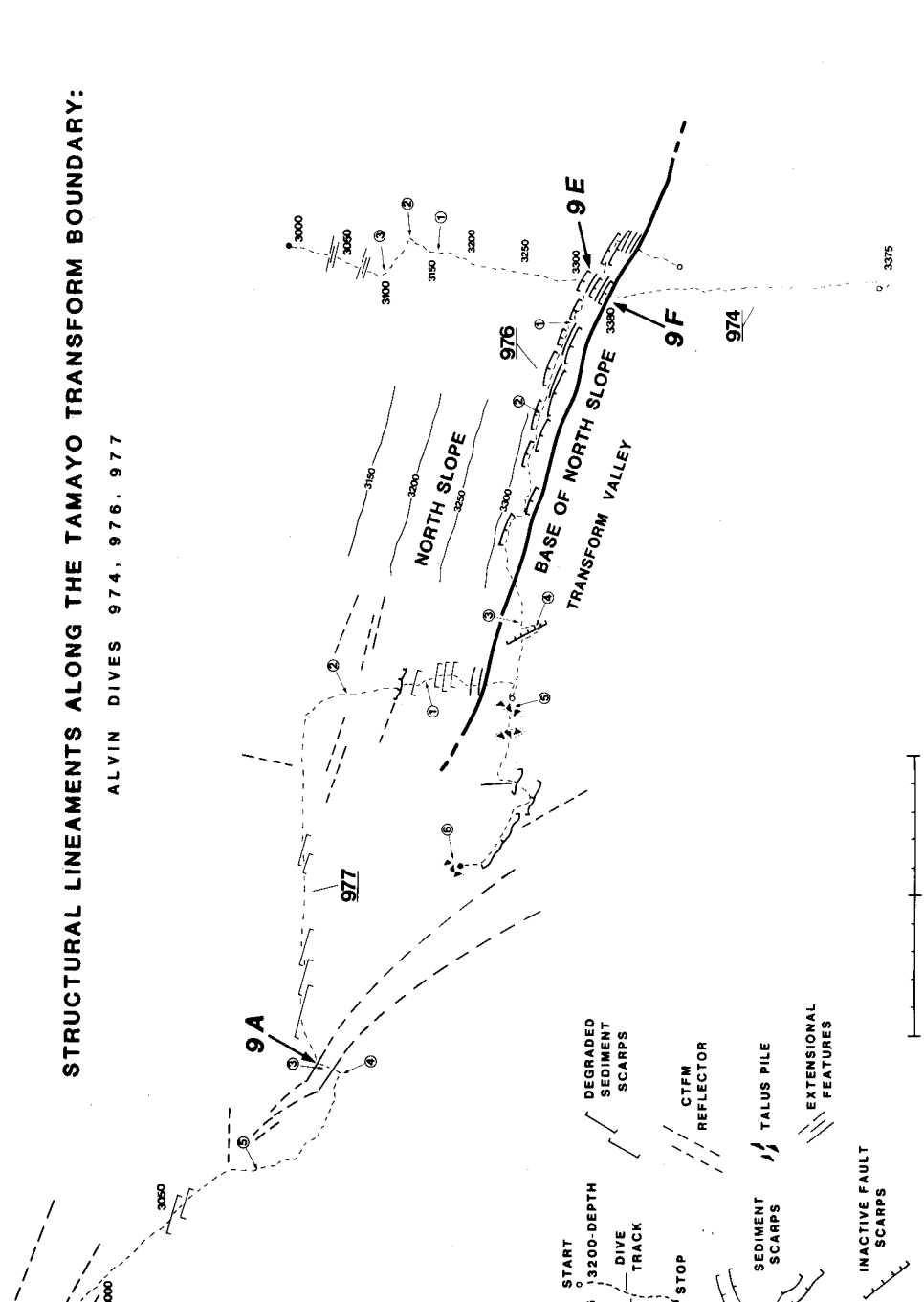

Fig. 6. Structural lineaments and geology along Dives 974, 976, 977 (location given in Figure 3). Inactive-fault scarps in volcanic basement trend obliquely while sediment scarps trend subparallel to the Tamayo Transform valley. Circled numbers indicate sampling locations. Bold numbers indicate locations of photos given in Figure 8 and 9.

bow camera photos show angular talus fragments and a possible source outcrop of volcanic rock as a small sill (~ 1 m thick) in the sediment. Apart from this example, no evidence of recent igenous activity was seen anywhere on the slope. In some instances the scarp faces expose laminations comprised of fine sands, silts and muds that are similar in appearance to the structures and relationships seen within the large disrupted blocks found on Dive 971 at the base of the sediment slope. Samples of this sediment were recovered from several localities along the slope and are composed of matrix-rich lithic and feldspathic sands that are finely laminated with lutites. The sands contain abundant angular quartz grains and contain lesser amounts of lithic particles, feldspar grains, and calcareous biogenic material. Analysis of the faunal assemblages indicate that the sediments are rich in Pleistocene to Quaternary benthic and pelagic assemblages, and that many of the benthic faunas are characteristic of relatively shallow water marine environments (shelf and upper slope), and therefore are suggestive of down slope displacement and resedimentation (personal communication: A. Boersma, W. Ruddiman, and M. Aubry). At some outcrops the scarps expose rubbly chaotic beds (~ 1 m thick) interlayered with the finely bedded arenites and lutites. The chaotic horizons observed in outcrop seem to be largely confined to the lower scarps. These chaotic beds are probably debris flows formed in the same way as those seen at the present base of the slope, re-exposed by tectonic activity.

The faces of scarps along the sediment slope typically show scalloped failure surfaces, and are corrugated by erosional rills and gullies along which the downslope movement of unconsolidated sediment occurs (Figures 9D, E, F). Along the base of individual sediment scarps, accumulations of talus are observed (Figure 9B) and consist of small sediment blocks and clods imbedded within a matrix of sedimentary material, partly hemipelagic, and similar in style to that of the more developed sedimentary wedge seen at the base of the sediment slope along Dive 971. Large detached slabs of manganese encrusted sediments (~ 4 m wide, < 2 m thick) are seen near the crest of some of the scarps along the sediment slope. All stages in the formation of these loose 'mega-blocks' are observed from nascent failure surfaces, represented by extensional gashes (see Figures 6, 7A; Dive 974) to individual sedimentary slabs found just downslope from their failure surfaces, to the large, mass wasted blocks found at the base of the sediment slope along Dive 971. Clearly, the sediment slope in this area is at least presently gravitationally unstable, and we infer that it is being tectonically disrupted.

Observations made during Dive 971 (Figures 4, 5A) show that the zone of active scarp degradation seen on the part of the slope crossed by that dive has a width, proximal to the ridge/transform intersection, of 1.5 km. Curiously, observations from Dives 974, 976, and 977 indicate that this zone, characterized by a series of steep, scalloped scarps, erosional gullies, and wedge-shaped debris deposits, becomes less prominent to the west (Figures 3, 6, 7). The total width of the disturbed terrain seen along Dive 974 was 250 m; along Dive 976, 150 m; and at the beginning of Dive 977, 100 m (Figures 6, 7). Farther to the west, in the middle

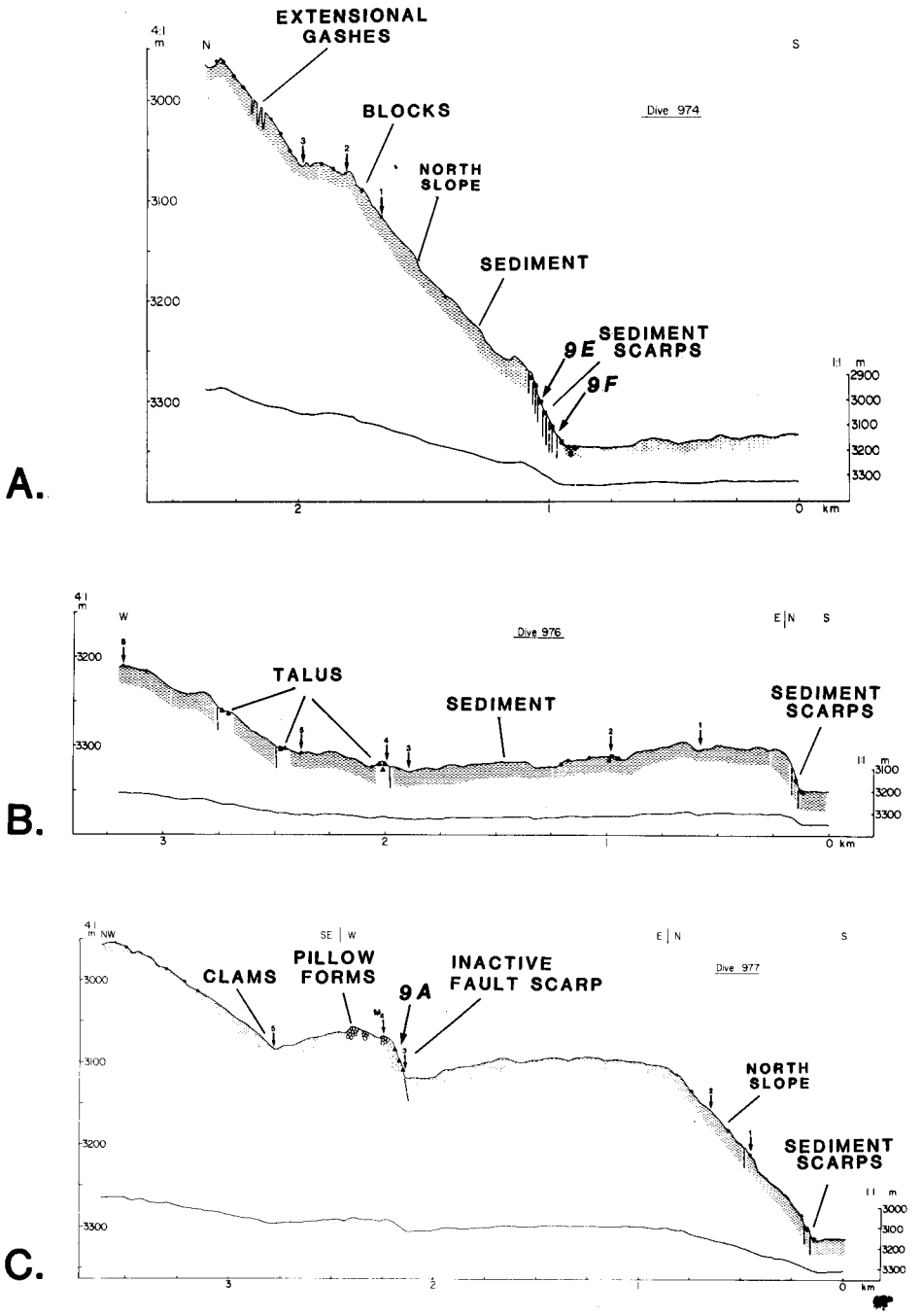

Fig. 7A–C. Geologic profiles and sampling locations (numbers above profiles) along Dives 974 (A), 976 (B), 977 (C) respectively (locations shown by Figure 3). 4:1 and 1:1 profiles are given for each dive. Symbols used for geology are identified for each profile. Bold numbers indicate locations of photos given in Figure 8 and 9.

and near the end of Dive 977 the zone of active mass wasting is not present at all along the base of the sediment slope. Instead, there are some smoothed-out, much degraded scarps (middle of Dive 977; Figure 7C) or none (near end of Dive 977). At the base of the north slope, near the end of Dive 977, a small, single area a couple of meters across was found in which a community of large clams existed. Most but not all of the creatures appeared to be dead; some had formed prominent trails in the mud bottom away from the area of greatest concentration. A small pit in the mud about 20 cm deep and 50 cm across next to the community contains what may be a small hydrothermal vent construction. The small size of the community suggests that the discharge was small and the moribund nature of the community suggests that the discharge is waning.

Dives 971 and 974 traveled perpendicular to the trend of the slope and the scarp trends, while Dive 976 and Dive 977 traveled, in part, parallel with the trend of the zone of active scarp degradation in order to examine individual scarps for continuity. Dive 976 (Figures 3, 7) traced a particular set of scarps for a distance of about 1.5 km along the transform valley and documented that these scarps are similar in location, trend and continuity to those defined by side-looking sonar data (Macdonald *et al.*, 1979). The scarp faces in this area are irregular, being disrupted and scalloped by local slope failure processes. Sediment scarp height within the more western area (Dives 974, 976, 977) is about the same as to that seen to the east along Dive 971 (~ 5 m), but the frequency of scarps in the zone in which they are developed in the western area seems to be greater (3–4 m) than that along 971, and nowhere are large, loose sedimentary slabs seen on slopes, nor are the sedimentary debris wedges at the base of scarps nearly as well developed (in areal extent or in size of blocks) as those seen towards the east opposite the EPR/Tamayo intersection (Dive 971). In fact, the lack of a significant debris wedge compared to the adjacent height and width of the zone of escarpments (see Figures 5A, 7A, 7B, 7C) on Dives 974, 976 and 977, and on Dive 971 is a key piece of evidence demonstrating that these are not the head scarps of rotational landslips. In the case of the three more western dives, the occurrence of these recent scarps at the base of the northern slope of the intersection depression requires that they cannot be landslide scarps and that they must be the surface expression of faults. The same argument applies to at least the lower scarps seen on Dive 971. Those seen higher on the slope during this dive cannot be so definitely identified as fault surface breaks on this criterion alone, although we think it is likely that they are, considering the overall geometry and distribution of the scarps and the debris derived from them (see Figures 5A, 7, 10b). A few small, north-facing scarps (~ 1 m high) were observed near the beginning of Dive 977 at the upper part of the zone of scarps and along the mid-section of Dive 976.

Above the zone of active scarp degradation described along Dives 974, 976, and 977, the south facing sediment covered slope is relatively undisturbed (Figures 3, 6, 7). Actively degrading sediment scarps of the size and style observed on the lower slopes are not seen, and the hemipelagic sediment-covered slope is only

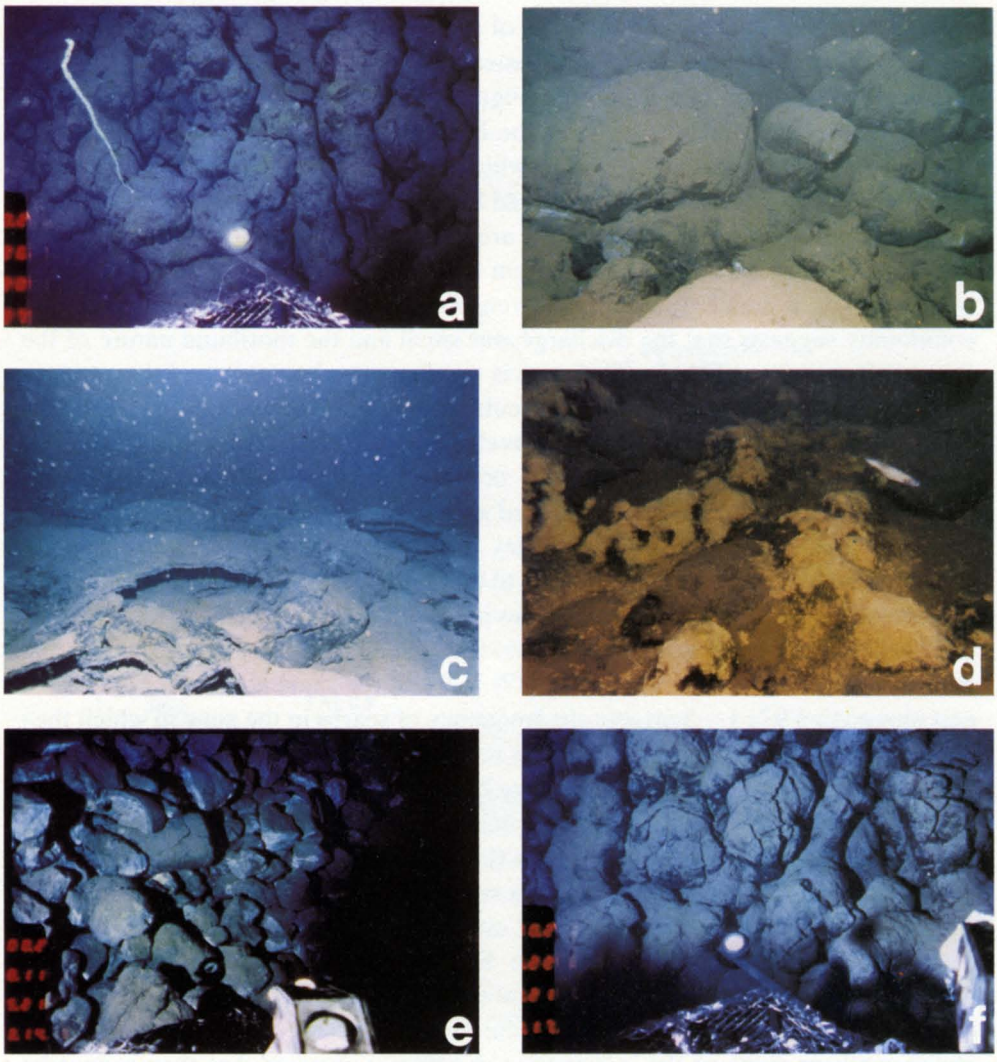

Fig. 8. Selected photographs of young volcanic terrain of the EPR. (A) Lightly sedimented pillows and tubular lava cylinders draping the flank of volcanic ridge located along EPR inner valley floor (Dive 975; time 17:54:20, depth 3188 m). (B) Lightly sedimented pillows and tubular lavas of the EPR inner-valley floor (Dive 975; time 17:19:09; depth 3179 m). (C) Thin (2–4 cm) veneer of flow overlying pillow forms (Dive 975; time 17:10:19; depth 3179 m). (D) Fluffy yellow-white precipitate interpreted to be of hydrothermal origin (Dive 975; time 18:10:03; depth 3203 m). (E) Fresh, sediment-free talus ramp at the base of a small (< 5 m) vertical offset fault scarp (Dive 975) indicative of recent tectonic activity and subsequent mass-wasting (Dive 975; time 21:13:14; depth 319 4m). (F) Relatively sediment-free, glass encrusted tubular and elongate pillow lavas seen high on the Western Rift valley wall suggesting a recent episode of off axis volcanism (Dive 972; time 21:53:17; depth 3325 m).

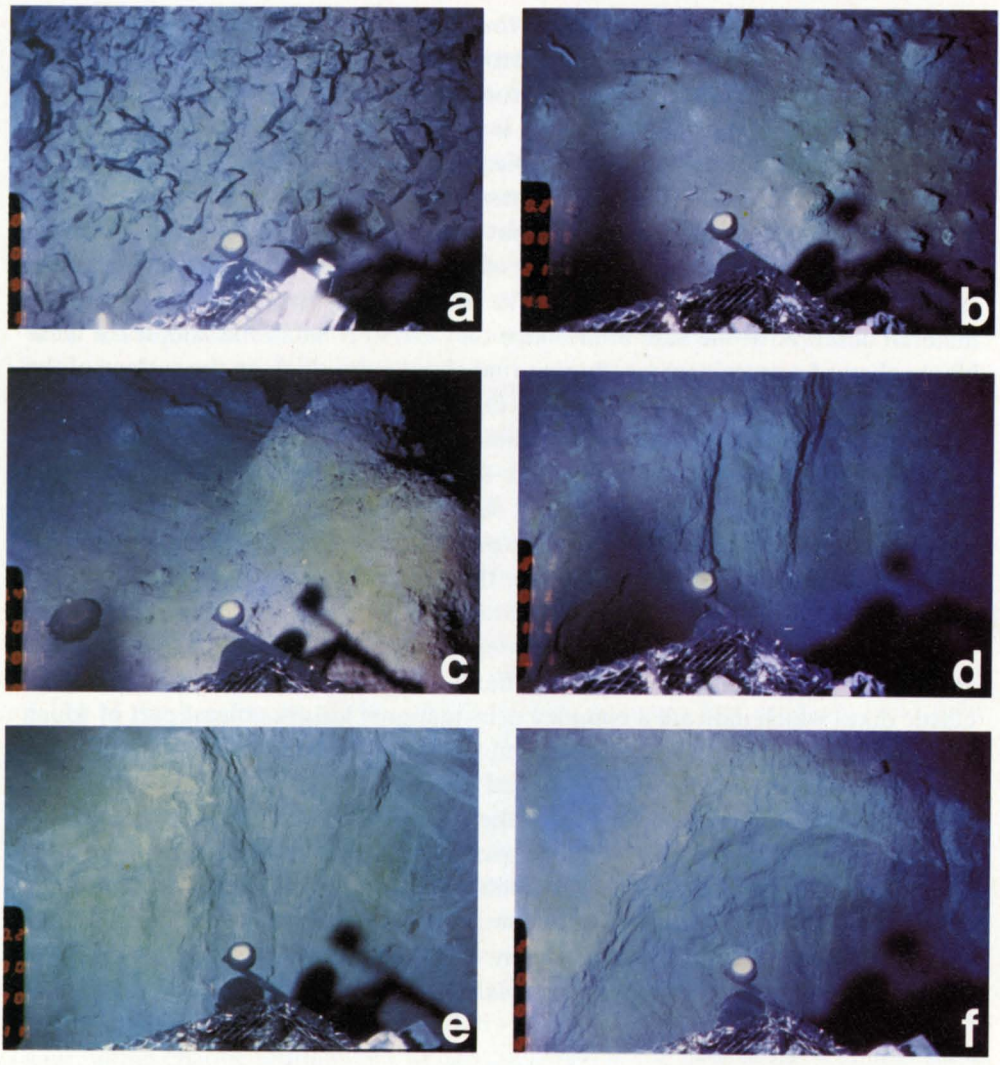

Fig. 9. Selected photographs of older volcanic terrain and north side of the intersection depression. (A) Talus ramp seen 9 km west of the EPR axis at the base of a N–S trending fault scarp. Managanese veneer and sediment cover suggests that this fault has been inactive for some time (Dive 972; time 19:12:21, depth 3082 m). (B) Debris wedge seen at the base of sediment scarps along the north side of the EPR-Tamayo intersection depression (Dive 971; time 21:54:49; depth 3260 m). (C) Larger (~ 1 m across) semi-consolidated sediment block in debris wedge at base of sediment scarps (Dive 971; time 20:29:10; depth 3435 m). (D) Scarps (< 2 m high) in semi-consolidated sediment showing corrugation of the scarp face. Scarp trend is approximately transform parallel (Dive 971; time 21:48:33; depth 3282 m). (E) Scarp face (< 2 m high) in semi-consolidated sediment showing erosional rills and lenses of lighter colored sedimentary material (Dive 974; time 20:35:11; depth 3315 m). (F) Scarp in semi-consolidated sediment showing 'scalloped' failure surface (Dive 974; time 20:31:22; depth 3323 m).

locally distorted by low amplitude, well-rounded sediment-covered benches which appear to be some type of inactive and eroded scarps in sediment. Although there is no evidence for recent faulting, throughout most or all of this area loose, sediment-veneered blocks are found scattered across and embedded in the hemipelagic blanket. The blocks are typically 10–50 cm in diameter and consist of either lithified sediments or weathered basalt. These blocks are widely spaced and some parts of the slope traversed do not show them; where they are seen, one might be observed in about 100 meters of traverse. Some of them are crumbling and disaggregating *in situ*, along cracks in the lithified rock, unlike the softer material observed at the base of the slope on Dive 971. All of the samples of these blocks showed a prominent weathering rind about 1 cm-thick on the surface of the block exposed to the water and next to cracks leading away from these surfaces. The extent of this weathering and the minimal hemipelagic coating on the blocks suggests that they have been exposed *in situ* for a significant time and that persistent winnowing of the hemipelagic material takes place along this part of the slope. The source area of these blocks, particularly those consisting of basalt, is presently unclear, although it is possible that fault scarp sources up-slope are not apparent due to a combination of tectonic and perhaps erosional degradation. Thin-section examination of a consolidated sedimentary block collected from this area, shows the presence of small microfaults ($\sim$ 1 cm offset) and associated small clastic dikes which indicate a complex deformational history at least part of which may have been of a surficial, soft sediment type. Another shows a complex network of cracks 1–2 mm wide filled with lithified micritic sediment, and has a surface on the base of the block showing low-relief 'slickensides-type' fabric defined by fibrous cryptocrystalline silica. This sample demonstrates derivation from a source where both brittle deformation and infiltration by initially soft sediment could occur. A few small incipient fissures, a few meters long and a centimeter or two wide, subparallel with the transform trend, were observed high on the slope on Dive 974 (Figure 7A). The significance of the isolated occurrence is not clear.

4. Discussion

4.1. The location of the principal transform displacement zone (PTDZ)

The trend, location and distribution of recently active scarps along the south facing sediment slope that bounds the north side of the EPR-Tamayo intersection depression suggest that this zone of instability reflects strike-slip deformation within the underlying volcanic basement and marks the location of the PTDZ. The orientation of the zone of scarp development and active mass wasting is roughly parallel with the regional trend of the Tamayo Transform (120°), the scarps represent the only sites of active transform-parallel deformation observed west of the EPR/Tamayo intersection area during our field program, and these structures, if extrapolated 20 km to the west along the transform valley, are coincident with a

deformed zone found by the submersible CYANA (CYAMEX and Pastouret, 1981). Although we documented abundant evidence for recent scarp development and slope modification, no field relationships were observed that demonstrate strike-slip displacements along the scarps. The structures observed along the sediment slope probably represent gravitationally induced erosional degradation of a free standing sediment wedge that is underlain by oceanic basement disrupted by strike-slip faulting.

It is interesting to note that when the along-strike perspective is considered, the character of the zone of slope instability changes markedly over a distance of 10 km. At the eastern end of our field area, opposite the EPR-tamayo intersection, the disturbed and disrupted terrain is over one kilometer wide. Towards the west the frequency of scarp development increases but the width of the disturbed zone is only about 100 m. We suggest that the apparent along strike change in the intensity of deformation is a function of the plate boundary geometry and kinematics of the transform. The turbidites and intercalated hemipelagic lutites sampled from scarps along the sediment slope were deposited on the floor of the Tamayo Transform at deposition centers located to the west within the northern trough. Subsequently, these deposits have been transported eastwards along the southern edge of the North American plate until they are exposed along the relatively deep closed-contour depression of the EPR-Tamayo intersection. As the sedimentary wedge moves from west to east along the intersection depression the depth to the floor of the depression increases, slope instability is enhanced because of continued transform tectonism, and deeper intervals of the sediment wedge are exposed as the relief of the slope increases (Figure 10A, B).

4.2. Structure and tectonic implications of the EPR-Tamayo intersection terrain

The orientation of fissures and small throw faults observed during the dive traverses (Dives 971, 972, 973, 975; Figure 4) located proximal to the EPR-Tamayo intersection clearly show that the most frequently observed structural trend is N–S (000°) and represents a structural fabric 30° oblique to the strike of the EPR axis (030°) and 60° oblique to the trend of the Tamayo Transform (120°). Farther to the west of the intersection, observations made during Dive 977 (Figure 6) document that structures located within a few kilometers of the PTDZ have orientations ranging from 350° to 000°. These structural data are all located within 5 km of the PTDZ and do not suggest a well-defined systematic change in orientation of structures with increasing proximity to the transform boundary. However, when these structural observations are integrated with the more regional perspective provided by deep-tow side-scan sonar data (Macdonald *et al.*, 1979; Figure 3) and regional bathymetry (Lewis *et al.*, 1983; Figure 3), there is a systematic change in the orientation of rise-axis parallel structures as the transform is approached and this pronounced change in orientation takes place about 5 km from the transform boundary. Previous investigations (Courtillot *et al.*, 1974;

Crane, 1976; Lonsdale, 1978; Searle, 1979; Macdonald *et al.*, 1979) of ridge-transform intersections have identified oblique trends but it remained to be established whether these structures represent faults that accommodate strike-slip displacements (Riedels, Anti-Riedels, secondary shear) or whether these structures are just oblique trending normal faults. The resolution of this ambiguity is crucial to an understanding of the tectonics of ridge-transform intersections. If the oblique faults largely accommodate strike-slip motion, then the intersection area encompassing the oblique structures is taken to represent a broad shear zone with strike-slip displacements distributed on numerous fractures. Continental analogues suggest that with time and continued displacement strike-slip motion would be focussed on a few faults which coalesce along strike to form a narrow shear zone (Tchalenko, 1970). Alternatively, if the oblique structures accommodate only or dominatly dip-slip displacements then these oblique trending normal faults simply reflect a distortion of the ridge axis extensional stress regime due to proximity to the strike-slip stress field generated along the transform boundary (Crane, 1976; Lonsdale, 1978; Searle, 1979; Macdonald *et al.*, 1979; Courtillot *et al.*, 1974).

Direct observation of these oblique structures during ALVIN traverses shows that the fissures do not accommodate large amounts of strike-slip displacements; the observations do not rule out a strike-slip component on these features much subordinate to the amount of extension. All fault-generated scarps observed on the dives in the extrusive terrain are degraded by varying degrees of mass wasting. It is therefore impossible to say with certainty (for example, by observing offset volcanic forms, or slickensides) that no strike-slip component of motion has occurred on these faults. However, the significant changes in orientation inferred for these faults along strike are more compatible with dominantly normal fault kinematics, as is their local parallelism with fissures (e.g. Dives 972, 975; Figures 4, 5). Furthermore, these faults are active at the ridge-transform boundary but are inactive (sediment-covered talus) to the west. Our dive observations support the notion that these oblique structures are the product of episodes of extension and that they do not accommodate significant amounts of strike-slip displacement and do not represent secondary shear within a broad zone of shear (Figure 10). This interpretation is consistent with models proposing that these structures result from the influence of a transform generated shear couple (Courtillot *et al.*, 1974; Crane, 1976; Lonsdale, 1978; Searle, 1979; Macdonald *et al.*, 1979; Gallo *et al.*, 1980).

It has recently been suggested that the oblique normal faults that are observed to disrupt the brittle volcanic skin of the oceanic crust is caused by a shear couple that forms at the ridge-transform intersection in the underlying upper mantle (Fox and Gallo, 1982; 1983). The juxtaposition of a cold edge of lithosphere against the truncated axis of an accreting plate boundary at a ridge-transform intersection cools the asthenosphere rising beneath the intersection and a mantle weld forms in the young lithosphere across the transform boundary. With continued sea floor spreading the weld deforms, creating a shear couple at the ridge-transform intersection which distorts the orientation of the axis of maximum tensile stress and

leads to the creation of normal faults and fissures with trends that are oblique to the overall direction of sea floor spreading.

The juxtaposition of a cold edge of lithosphere against an accreting plate boundary will also restrict the amount of partial melting which may occur in the rising asthenosphere at the ridge-transform intersection (Gallo and Fox, 1979; Stroup and Fox, 1981; Fox and Gallo, 1984). The production of smaller volumes of basaltic melt per unit time predicts that the crust should thin in the vicinity of ridge-transform intersections and that the underlying upper mantle should be heterogeneous. Seismic refraction studies (McClain and Lewis, 1980) indicate that the thickness of the oceanic crust thins by 2 to 3 km in the vicinity of the Tamayo Transform boundary. Furthermore, modeling of geochemical data from the analyses of basalts recovered in this project from along the axis of the EPR south of the Tamayo Transform demonstrate that the basalts created in close proximity to the Tamayo Transform boundary are the products of relatively small amounts of

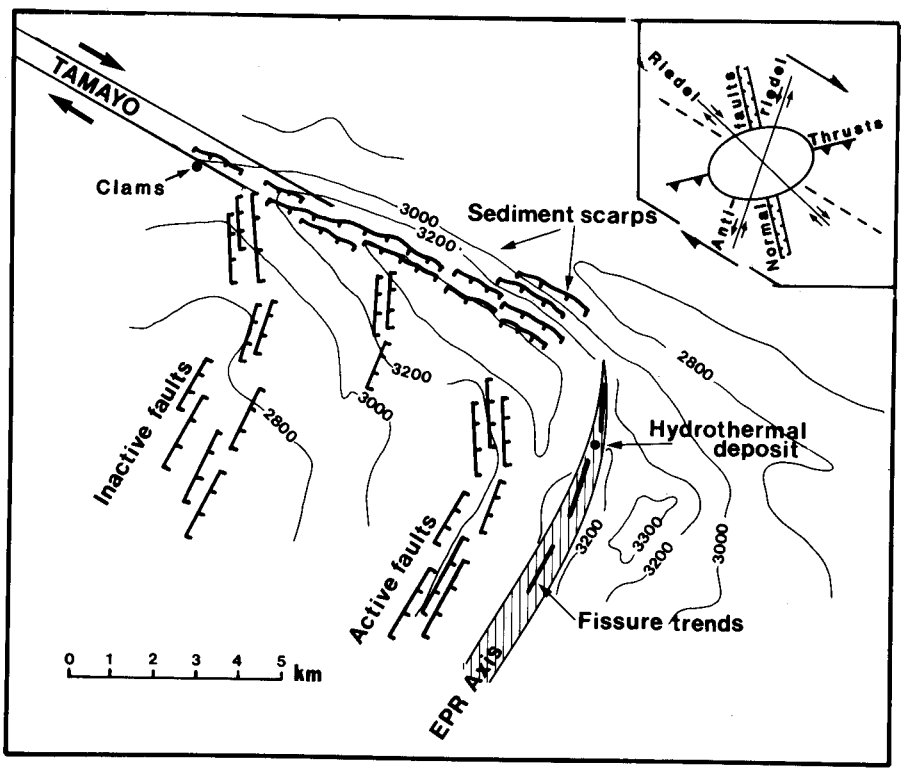

Fig. 10A. Schematic interpretation of the EPR-Tamayo intersection showing deflection of the EPR axis and fault and fissure trends as the Tamayo Transform is approached. Structures generated within a right-lateral shear couple are shown in insert (upper-right). Note that the volcanic terrain of the EPR axis protrudes across the Tamayo-EPR intersection depression. Sediment scarps on the north side of the EPR-Tamayo intersection are taken to represent strike-slip deformation in the underlying volcanic basement.

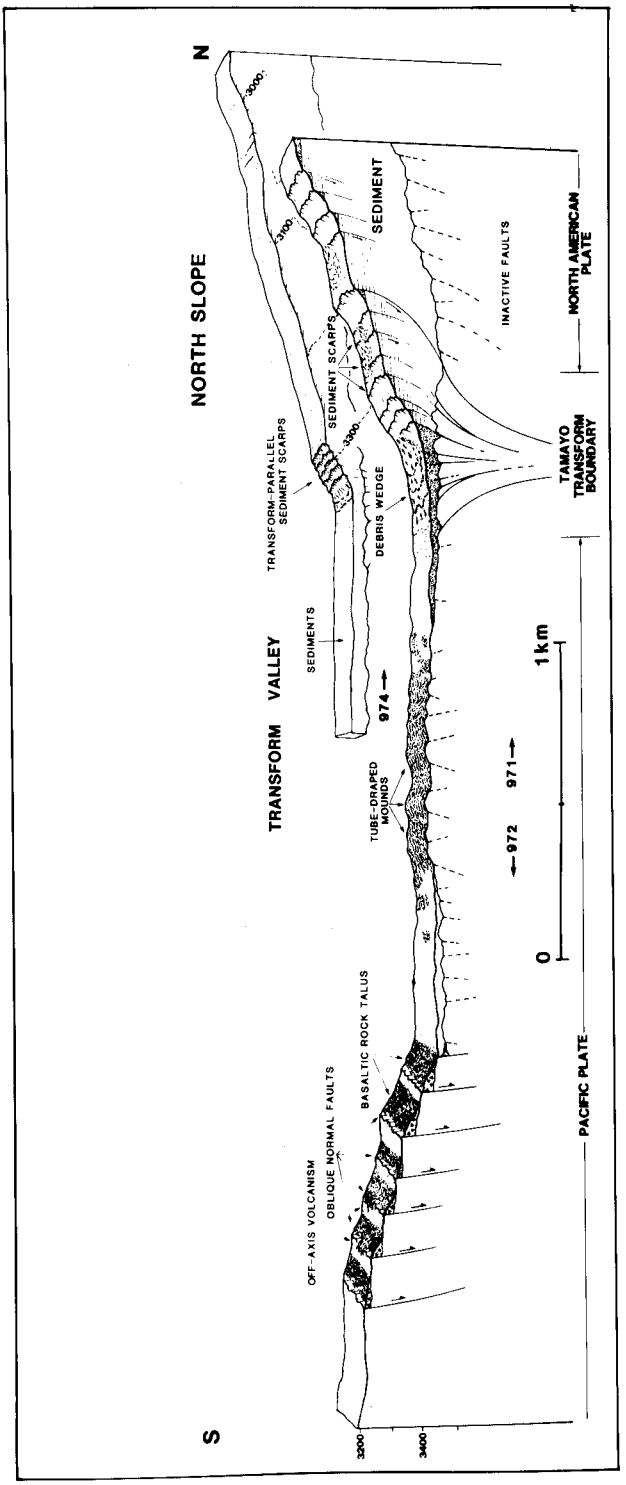

Fig. 10B. Schematic 3–D swath-profiles (compiled from Dives 971, 972, and 974) across the Tamayo Transform boundary showing observed relief, 'surface' geology and structure as well as interpretative basement geology.

partial melting; basalts sampled down the axis of the EPR away from the Tamayo Transform boundary indicate much higher degrees of partial melting (Bender *et al.*, 1981, 1984).

A further expression of the thermal effect of the transform can be seen in the progressive and systematic deepening of the axis of the East Pacific Rise as the transform boundary is approached over several tens of kilometers. This 700 m elevation difference may be due to a number of factors: the reduced thickness of the crust; a density gradient in the upper mantle caused by a descent of isotherms towards the transform and by a change in the composition of the upper mantle related to variable degrees of partial melting.

6. Concluding Remarks

The bathymetric and structural data collected during our 1979 investigation of the EPR-Tamayo intersection allows us to document some relationships that shed light on the processes that are responsible for shaping this type of tectonic terrain.

Rise axis constructional terrain can be traced down into and across the closed contour depression that defines the EPR-Tamayo intersection (Figure 10). Along the north side of the depression the volcanic basement disappears beneath a wedge of sedimentary talus that has been shed from actively eroding sediment scarps. These scarps are located along the lower portion of a 300 m to 600 m high sediment slope, they expose an interbedded assemblage of turbidites and hemipelagic lutites, and they define a narrow zone (100 to 1500 m) of active slope modification that can be traced along strike for a distance of 10 km. We suggest that this zone of active mass wasting and slope modification which trends 120°, approximately parallel to the North American plate-Pacific plate slip direction, marks the surficial location of the principal transform displacement zone (Figure 10). Strike-slip motion transports sediments of the north trough eastwards and exposes them on the northern flank of the intersection depression creating a gravitationally unstable edge of sediments that slump, fail and prograde out over the principal transform displacement zone. These deposits are in turn subjected to further tectonic erosion and mass wasting induced by strike-slip motion in the underlying volcanic basement.

Within about 5 km of the Tamayo Transform boundary, the dominant trend of faults and fissures created along the EPR is 000°; 60° oblique to the regional direction of sea floor spreading and 30° oblique to the axis of the EPR (Figure 10). All of the structures observed within the EPR/Tamayo ridge-transform intersection area are interpreted to accommodate primarily dip-slip motion. These data are consistent with models suggesting that oblique structures at ridge-transform intersections represent ridge-axis extensional regimes distorted by a shear couple (Courtillot *et at.*, 1974; Crane, 1976; Lonsdale, 1978; Searle, 1979; Gallo *et al.*, 1980) generated in the upper mantle beneath the ridge-transform intersection where newly formed lithosphere intermittenly welds to the cold edge of the transform boundary (Fox and Gallo, 1982, 1984).

Acknowledgements

We are indebted to the Masters, officers and crews of the research vessels LULU and GILLISS and especially to the pilots and technical support team of the Deep Sea Research Vessel ALVIN for their enthusiasm and dedication that kept the submersible operational making our science possible. We are grateful to J. F. Bender and C. H. Langmuir for providing insight to the petrologic character of the oceanic basalts generated proximal to transform boundaries and we thank them for a preprint of their paper. We thank D. J. Fornari and J. B. Stroup for constructive criticism of an early draft of this manuscript and K. Louden for his review of the final version. W. Ruddiman, A. Boursma, M. Aubry, and E. Pokras provided analyses of the faunal assemblages of the sediment samples and their help is gratefully acknowledged. This work was financially supported by the National Science Foundation under Grant Number OCE79-13144. WHOI cont. number 5488.

References

Bender, J. F., Hanson, J. N., and Langmuir, C. H.: 1981, 'Basalt Glasses from the East Pacific Rise-Tamayo Transform Intersection: Geochemical Evidence for Complex Magma Generation Processes', *Trans. Amer. Geophys. Union* **62**, 423.

Bender, J. F., Langmuir, C. H., and Hanson, J. N.: 1984, 'Petrogenesis of Basalts from the Tamayo Region, East Pacific Rise: Evidence that Partial Melting is Responsible for Systematic Variations in Glass Chemistry with Distance from a Transform Fault', *Jour. Petrol.* (in press).

Chinnery, M. A.: 1966, 'Secondary Faulting', *Can. Jour. Earth Science*, **3**, 163–174.

Courtillot, V., Tapponier, P., and Varet, J.: 1974, 'Surface Features Associated with Transform Faults: A Comparison Between Observed Examples and an Experimental Model', *Tectonophy*, **24**, 317–329.

Crane, K.: 1976, 'The Intersection of the Siquieros Transform Fault and the East Pacific Rise', *Mar. Geology* **21**, 25–46.

CYAMEX Scientific Team and Pastouret, L.: 1981, 'Submersible Structural Study of the Tamayo Transform Fault, East Pacific Rise at 23° N', *Mar. Geophys. Res.* **4**, 381–401.

Fox, P. J. and Gallo, D. G.: 1982, 'A Mantle Weld at Ridge Transform Intersections: Implications for the Development of Oblique Structures', *Trans. Amer. Geophys. Union* **63**, 446.

Fox, P. J. and Gallo, D. G.: 1984, 'A Tectonic Model for Ridge-Plate Boundaries: Implications for the Structure of Oceanic Lithosphere', *Tectonophysics* (in press).

Gallo, D. G. and Fox P. J.: 1979, 'The Influence of Transform Faults on the Generation of Oceanic Lithosphere', *Trans. Amer. Geophys. Union* **60**, 376.

Gallo, D. G., Rosencrantz, E. R., and Rowley, D. B.: 1980, 'Oblique Structures at Ridge-Transform Intersections: Implications for Ridge Dynamics and Pole Determinations', *Trans. An Geophys. Union* **61**, 358.

Karson, J. A. and Dick, H. J. B.: 1983, 'Tectonics of Ridge-Transform Intersections at the Kane Fracture Zone', *Mar. Geophys. Res.* **6**, 51–98.

Kastens, K. A., Macdonald, K. C., Becker, K., and Crane, K.: 1979, 'The Tamayo Transform Fault in the Mouth of the Gulf of California', *Mar. Geophys. Res.* **4**, 129–152.

Larson, R. L., Menard, H. W., and Smith, S. M.: 1968, 'Gulf of California: A Result of Ocean Floor Spreading and Transform Faulting', *Science* **161**, 781–784.

Larson, R. L.: 1972, 'Bathymetry, Magnetic Anomalies and Plate Tectonics History of the Mouth of the Gulf of California', *Geol. Soc. Am. Bull.* **83**, 3345–3360.

Lewis, B. T. R.: 1979, 'Periodicities in Volcanism and Longitudinal Magma Flow on the East Pacific Rise at 23° N', *Geophys. Res. Lett.* **6**, 753–756.

Lewis, B. T. R., Syndsman, W. E., McClain, J. S., Holmes, M. L., and Lister, C. R. B.: 1983, 'Site Survey

Results at the Mouth of the Gulf of California, Leg 65', *Deep Sea Drilling Project, Init. Repts. DSDP* **65**, 309–323.

Lonsdale, P.: 1978, 'Near-Bottom Reconnaisance of a Fast-Slipping Transform Fault Zone at the Pacific-Nacza Plate Boundary', *Jour. Geol.* **86**, 451–472.

Macdonald, K. C., Kastens, K., Spiess, F. M., and Miller, S. P.: 1979, 'Deep-Tow Studies of the Tamayo Transform Fault', *Mar. Geophys. Res.* **4**, 37–70.

McClain, J. S. and Lewis, B. T. R.: 1980, 'A Seismic Experiment at the Axis of the East Pacific Rise', *Mar. Geol.* **35**, 147–170.

McKinstry, H. E.: 1953, 'Shears of the Second Order', *Amer. Jour. Sci.* **251**, 401–414.

OTTER Scientific Team: 1984, 'The Geology of the Oceanographer Transform: The Ridge-Transform Intersection', *Mar. Geophys. Res.* **6**, 109–141 (this issue).

Riedel, W.: 1929, 'Zur Mechanic Geologischer Brucherscheinungen', *Zentralb. Mineral. Geol. Pal.* 1929B, 354–368.

Searle, R. C.: 1979: 'Side-Scan Sonar Studies of North Atlantic Fracture Zones', *J. Geol. Soc. London* **136**, 283–293.

Stroup, J. B. and Fox, P. J.: 1981, 'Geologic Investigations in the Cayman Trough: Evidence for Thin crust along the Mid-Cayman Rise', *J. Geol.* **89**, 395–420.

Tamayo Scientific Team: 1980a, 'Tectonics of a Ridge-Transform Intersection Zone: Tamayo-East Pacific Rise, Gulf of California, *EOS. Trans. Amer. Geophys. Union* **61(32)**, 574.

Tamayo Scientific Team: 1980b, 'Submarine Landsliding at the Eastern End of the Tamayo Transform Fault, Gulf of California', *EOS, Trans. Amer. Geophys. Union* **61(17)**, 359.

Tamayo Scientific Team: 1980c, 'East Pacific Rise-Tamayo Transform Fault Intersection', *Geol. Soc. Amer. Abstracts with Programs* **12(7)**, 461–462.

Tchalenko, J. S.: 1970, 'Similarities between Shear Zones of Different Magnitudes', *Geol. Soc. Am. Bull.* **81**, 1625–1640.